Materials and Design 161 (2019) 106–113

Contents lists available at ScienceDirect

Materials and Design

journal homepage: www.elsevier.com/locate/matdes

Effect of solid phase corrugation on the thermo-mechanical properties of low density flexible cellular polymers

S. Pérez-Tamarit [a,*], E. Solórzano [a], A. Hilger [b], I. Manke [b], M.A. Rodríguez-Pérez [a]

[a] Cellular Materials Laboratory (CellMat), Condensed Matter Physics Department, Science Faculty, University of Valladolid, Paseo de Belén, 7, 47011 Valladolid, Spain
[b] Helmholtz-Zentrum Berlin fürMaterialien und Energie, Lise-Meitner-Campus, Hahn-Meitner-Platz 1, 14109 Berlin, Germany

HIGHLIGHTS

- The corrugation of the solid phase of a collection low density cellular polymers was calculated by image analysis.
- Two image analysis protocols were developed and applied in high resolution synchrotron X-ray tomographies.
- The corrugation is the responsible of the decrease of experimental collapse stress from its ideal theoretical value.
- The thermal expansion coefficient suddenly increase at 25 °C due to solid phase corrugation.

GRAPHICAL ABSTRACT

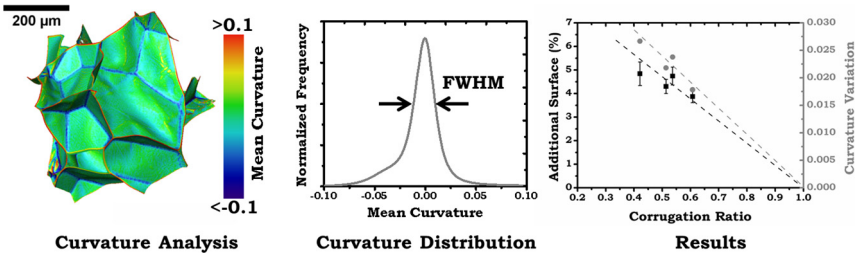

ARTICLE INFO

Article history:
Received 31 July 2018
Received in revised form 6 November 2018
Accepted 7 November 2018
Available online 9 November 2018

Keywords:
Synchrotron tomography
3D analysis
Cellular polymers
Solid phase corrugation
Collapse stress
Thermal expansion coefficient

ABSTRACT

This manuscript presents the effect of the solid phase corrugation of low density flexible cellular polymers on both their mechanical and thermal properties. First, a detailed quantification of solid phase corrugation has been carried out by means of high resolution synchrotron micro-tomography in a collection of polyethylene foams. Subsequently, the collapse stress in compression has been analysed both from the theoretical and experimental points of view achieving a clear relation between the solid phase corrugation and the ratio of theoretically calculated and experimentally measured collapse stress. Finally, solid phase corrugation has been correlated with the thermal expansion coefficient at room temperature.

1. Introduction

Cellular polymers are biphasic materials in which a gaseous phase is dispersed into a solid phase [1]. As a consequence, the final physical properties of cellular polymers depend, on the one hand, on the amount of gas and its distribution throughout the structure, and, on the other hand, depend on a set of characteristics of the solid phase. Its tuneable structure has allowed cellular polymers becoming a good solution in a wide range of applications in several market sectors such as automotive, packaging, building, etc.... [2]. In particular, low density flexible cellular polymers are characterized by relative densities lower than 0.1 and consequently solid architectures owning very thin cell walls (2–4 μm) [3,4]. The low stiffness of the matrix polymer, the mentioned thin solid architecture and other factors, such as the reduced inner gas pressure, may cause the presence of wrinkles on the cell walls leading to an overall corrugation of the solid phase (Fig. 1) [3]. Fig. 1 shows tomography slices of two low density flexible polymers. Fig. 1(a) shows the structure

* Corresponding author.
E-mail address: saul.perez@fmc.uva.es (S. Pérez-Tamarit).

https://doi.org/10.1016/j.matdes.2018.11.020

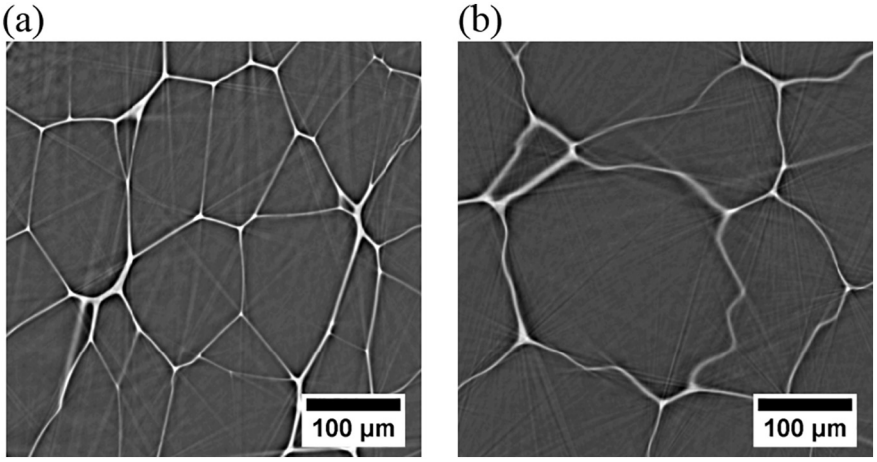

Fig. 1. Tomographic slices of low density cellular polymers with (a) solid phase with flat cell walls and (b) corrugated solid phase.

of a sample with flat cell walls while Fig. 1(b) shows a foam in which cell walls present a significant degree of corrugation (i.e. the cell walls present wrinkles).

Low density flexible cellular materials are used to package fragile products against impact damage during transportation and in body protection such as helmets, knee pads, shin guards, etc. [5–7]. For this reason, the mechanical behaviour in compression is one of the most important properties of these materials [8]. Therefore, abundant scientific investigations have been focused on studying the compression behaviour of low density cellular polymers since 1959. Most of these theories consider that mechanical response depends on a multitude of parameters such as relative density, cell size, fraction of material in the foam edges and open cell content and pressure of the gas in cells [9–11]. However, few studies have been carried out in order to understand the effect of the solid phase corrugation on the mechanical properties due to the challenging fact of measuring this structural parameter [12,13].

In fact, it is well known that the presence of wrinkles in a flat surface reduces the required force need to buckle it, in comparison with a totally flat surface [14]. In the case of low density cellular polymers, little imperfections in the solid phase can reduce the collapse stress of the samples, which is a critical mechanical parameter for the application of these materials [15]. Therefore, investigating the exact influence of solid phase corrugation is crucial in order to manufacture optimum materials for the above-mentioned applications.

For this purpose, the first step consisted on developing accurate and robust characterization methods to determine the solid phase corrugation. Due to the reduced cell wall thickness of the selected samples we have used synchrotron μ-CT data sets to obtain information from the cell walls at this resolution level [12,16]. The information about solid phase corrugation has been obtained by self-developed methods, some of them requiring time-consuming algorithms (Section 2.3). The influence of solid phase corrugation on the collapse stress is determined by comparing both experimental and theoretical values of this parameter (Section 2.4). The influence of solid phase corrugation on thermal expansion has been also analysed in this investigation by comparing the slope of the expansion coefficient at 25 °C (Section 2.5). It is well known that the thermal expansion coefficient of this type of cellular polymers is influenced by the solid phase corrugation [3]. However, this influence was not studied in detail before due to the inherent difficulty of characterizing accurately this structural parameter.

Consequently, the main objective of this investigation is to determine the solid phase corrugation (presence of wrinkles in the cell walls), validate the indicators developed in this investigation and quantify the effect of solid phase corrugation on thermo-mechanical properties (collapse stress and thermal expansion coefficient) of low density flexible cellular polymers. To this end, four cellular polymers based on a flexible polymer matrix fabricated by a foaming process which induces corrugation in the cell walls (Section 2.1) have been used.

2. Experimental

2.1. Materials

The materials involved in this investigation are cross-linked closed-cell cellular polymers manufactured by a high-pressure nitrogen gas solution process [2]. The raw material used wasa low density polyethylene (LDPE). In this process, an extruded sheet is irradiated and cross-linked and then placed in an autoclave. There, it is subjected to the high pressure of nitrogen gas at temperatures above the polymer softening point. Under these conditions, the nitrogen is dissolved into the polymer matrix. At the end of the solution stage and after cooling, the pressure is reduced to atmospheric pressure. Then, the materials are placed in a second low-pressure autoclave and again heated above the polymer melting point. The release of the pressure in this second step allows the full expansion of the polymeric material than can reach densities as low as 15 kg/m^3. Finally, the foamed slabs are cooled to room temperature. The foams produced by this technology are isotropic closed cell cellular polymers [17]. In this process, the reduction of temperature in the cooling step promotes a reduction of the gas pressure in the cells that results into a corrugation of the cell walls due to the low strength of the solid phase structure, composed of very thin cell walls (thickness 2–4 μm) [16] of a flexible polymer (LDPE). Some of the main descriptors of both the gas and solid phases for the materials under study have been measured using a multi-scale characterization based on X-ray tomography [18]. These structural characteristics have been summarized in Table 1.

2.2. Synchrotron X-ray μ-CT

Considering the reduced thickness of cell walls these samples (around 2–4 μm) [18], the analysed specimens were scanned using synchrotron X-ray micro-tomography (μ-CT) at BAMline (BESSY II synchrotron, HZB, Berlin) [19]. The specific conditions of the tomographic experiments in terms of low energy (9.8 keV), long exposure time (3000 ms), and number of projections (2200) allowed obtaining tomographic results with excellent contrast (Fig. 2 TOP). Further, the reached spatial resolution (0.438 μm of voxel size) permitted reconstructing the thinnest parts of the solid phase of all the tested cellular polymers (Fig. 2 BOTTOM). The tomography-scanned volumes corresponded to approx. 3 mm^3.

Table 1
Density and cellular structure characteristics of the cellular polymers under study.

Sample	Density (ρ_f) [kgm^{-3}]	Cell size (ϕ) [μm]	Coordination number (n_i)	Fraction of mass in struts (f_s)
LDPE-1	16.4 ± 0.4	310 ± 50	14.1 ± 3.3	0.117
LDPE-2	20.2 ± 0.5	270 ± 50	13.8 ± 3.1	0.122
LDPE-3	31.2 ± 0.8	260 ± 50	14.1 ± 3.0	0.176
LDPE-4	41.3 ± 0.5	340 ± 60	13.7 ± 3.1	0.390

2.3. Curvature analysis

We have selected two different methods to obtain quantifiable values of the solid phase corrugation.

On the one hand, several pores have been analysed calculating their volume and surface and directly obtaining their surface/volume ratio ($(S/V)^{cell}$) by using Avizo software package [20]. Then, since the cell geometry for this type of materials is mainly tetrakaidecahedral (average coordination number of 14 (Table 1), i.e. an average of 14 walls per cell) and the cells are isotropic [17,18], the surface/volume ratio has been normalized considering the surface/volume ratio of a regular Kelvin cell containing the same volume ($(S/V)^{Kelvin}$) [1,21]. The normalization of the surface/volume ratio allowed us to eliminate the influence of pore size in the surface/volume ratio values. Finally, the Additional Surface (*AS*) due to cell wall corrugation is calculated as expressed in Eq. (1).

$$AS(\%) = 100 \cdot \left(\frac{(S/V)^{cell}}{(S/V)^{Kelvin}} - 1 \right) \tag{1}$$

This simple parameter reveals differences between materials and seems to be a good indicator of the presence of wrinkles in the solid structure, as it will be shown in the results section. In fact, other works in the literature have dealt with a similar parameter but considering the equivalent sphere to normalize the S/V ratio of the cells finding values for *AS* around 120% (normalized S/N 2.2) [12]. Consequently, it is proved in this work that the election of the corresponding Kelvin cell as reference for normalization and the selection of *AS* as the representing parameters seems to be more appropriate.

On the other hand, a more complex method based on surface discretization by means of surface meshing has been used. It uses triangles and a method for local surface approximation by continuous mathematical functions [22–24]. Several geometrical parameters can be calculated from this analysis, all of them based on the two principal radii of curvatures of the surface, r_1 and r_2. Among all the possible curvatures definition (mean, maximum, minimum, Gaussian, etc) we have selected the mean curvature (C_a) as a quantifiable indicator of the presence of wrinkles. Mean curvature is defined in Eq. (2) as a function of the above mentioned radii.

$$C_a = \frac{1}{2}\left(\frac{1}{r_1} + \frac{1}{r_2} \right) \tag{2}$$

A negative value of the local mean curvature corresponds to strictly concave regions whereas local positive values of this parameter are located in strictly convex surfaces. The main advantage of computing mean curvature instead of Gaussian curvature is its wider distribution and higher sensitivity to local variations [25–27].

The curvature computation was carried out using Avizo software package [20]. The method uses a marching-cubes algorithm to create a triangular mesh in the cellular polymer structure surface [28–30]. This mesh is smoothed by an iterative computational process so the local pixel "roughness" is almost eliminated. Smoothing is accomplished by shifting the triangular vertexes to average positions, considering the neighbours. Maximum shifting of 50% (rather low value) and a high number of iterations (10) were the parameters considered to remove local variations without significantly modifying the original surface. The mean curvature analysis was accomplished considering a surface field including a significant number of neighbouring triangles. After proper optimization we considered 20 neighbouring triangles in the computations. The high compliance reached by using such neighbourhood conditions made it unnecessary to iterate and refine the mean curvature calculation. The typical computation time under these conditions was between 6 and

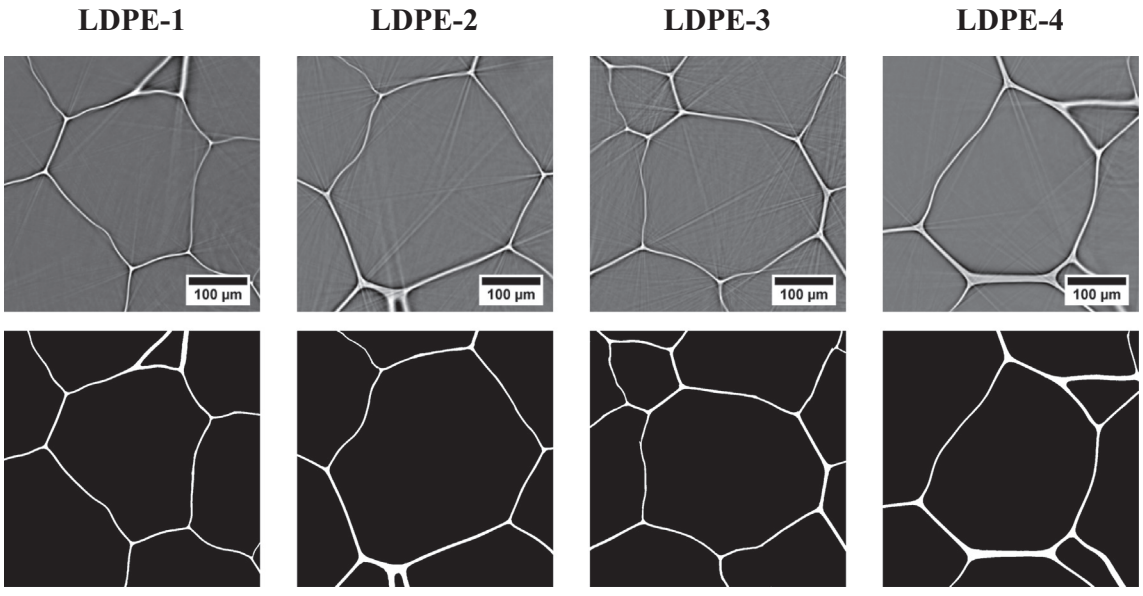

Fig. 2. Grey-level slices –TOP– and binarized slices –BOTTOM– for all the foam specimens under study.

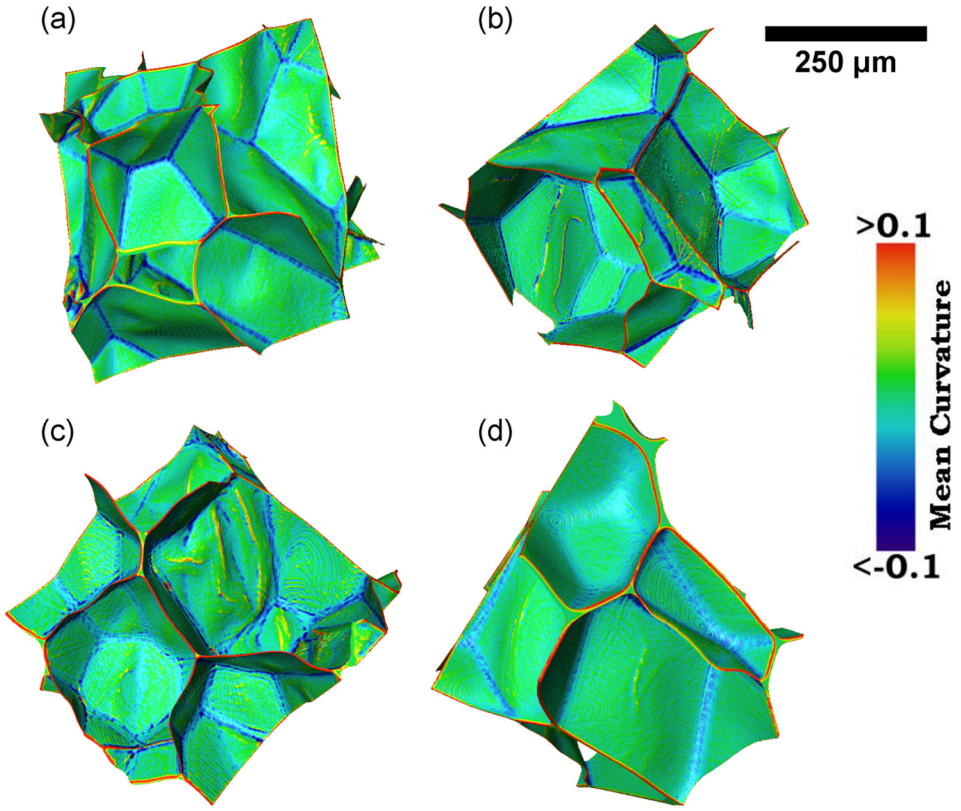

Fig. 3. Surface mean curvature maps for a volume of 900x900x900 voxels. (a) LDPE-1 (b) LDPE-2 (c) LDPE-3 and (d) LDPE-4.

8 h. In order to eliminate local effects in the different samples three different volumes of interest (900 × 900 × 900 voxels or 0.4 × 0.4 × 0.4 mm^3) were analysed obtaining similar results in all zones. The results for one of the analysed zones in each material are shown in Fig. 3. The final output is represented as histograms of mean curvature distribution using the same representation range and number of bins.

2.4. Collapse stress

One of the most critical physical properties of low density flexible cellular polymers is the collapse stress which is defined as the strain at which elastic buckling of the cell walls of the cellular materials occurs [31,32]. From a theoretical point of view this property depends on density, properties of the solid phase, cell geometry, fraction of material in the struts and corrugation of the solid phase [11]. However, this last parameter has never been considered in the traditional models described at the beginning of Section 2.4.1. It is expected that the presence of wrinkles on the cellular structure should lead to a significant reduction of collapse stress and therefore we have proposed a semi-empirical parameter which takes corrugation into account.

2.4.1. Geometrical modelling of collapse stress

Gibson and Ashby (1988) suggested an analytical model [1] to account for the collapse stress (σ_c) of cellular polymers (Eq. (3)). They considered isothermal conditions with short timescales, and hence no gas diffusion, in a cubic cell structure.

$$\sigma_c = E_s G\left(\rho_f/\rho_s\right)^2 \tag{3}$$

where ρ_f is the density of the cellular polymer, ρ_s is the density of the matrix polymer and E_s is the Young modulus of the solid polymer. In

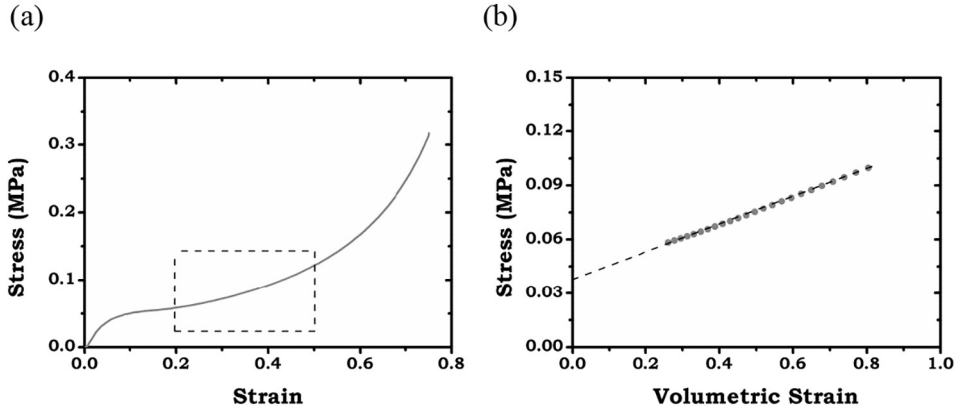

Fig. 4. Stress vs strain compression curve (a) and (b) stress vs volumetric-strain in the post collapse zone for sample LDPE-3.

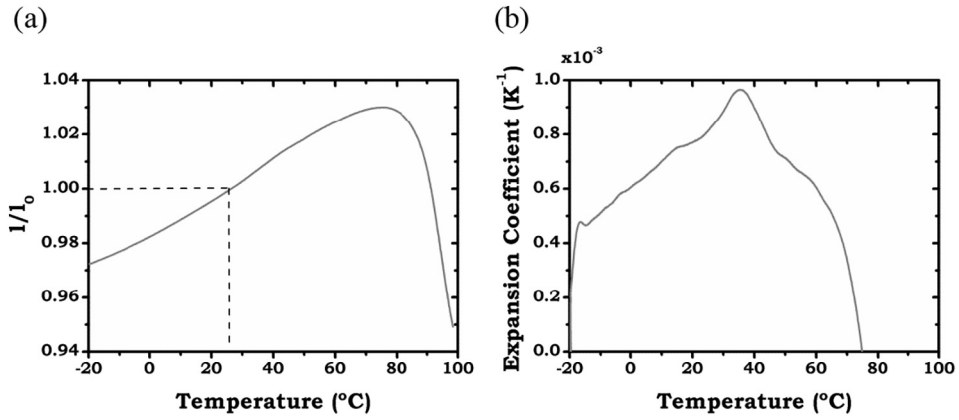

Fig. 5. (a) Normalized sample thickness (l/l_0) and (b) thermal expansion coefficient as a function of temperature for LDPE-1 sample.

addition, G is a geometric constant whose value, proposed by Gibson and Ashby, is 0.05.

But instead of using the simple cubic geometry a better approximation is reach if cells are modelled as tetrakaidecahedrons. In the case of a cell face with width w, side a and thickness δ, the compression force required to initiate the elastic buckling of a cell face (F_c) is given by Euler's formula:

$$F_c = \left(\frac{2\pi}{a}\right)^2 E_s \frac{w\delta^3}{12} \tag{4}$$

In addition, we need to take into account the relationship between the cellular structure characteristics and the cellular material density [1]:

$$\frac{\rho_f}{\rho_s} = \frac{C}{1-f_s}\left(\frac{\delta}{\phi}\right) \tag{5}$$

where C is a constant that depends on cellular geometry and f_s is the fraction of material in the struts. Combining Eqs. (4) and (5) the collapse stress can be described as follows:

$$\frac{\sigma_c}{E_s} = G\left(\frac{\rho_f}{\rho_s}\right)^2 = \frac{1}{12}\left[\frac{2\pi(1-f_s)B}{C}\right]^2\left(\frac{\rho_f}{\rho_s}\right)^2 \tag{6}$$

where B is a constant that condensates other geometric constants. Assuming that cells have the geometry of tetrakaidecahedrons the constants B and C can be calculated [1] taking the following values: $B = 2.828$ and $C = 3.348$.

Eq. (6) accounts for the collapse stress assuming flat cell walls. In order to introduce the solid phase corrugation the previous equation was modified introducing the so-called "corrugation ratio" (ξ) (Eq. (7)) [33]. This term is related to the cellular structure and more specifically to the presence of wrinkles in the cellular polymer structure. Further, this parameter varies between 0 and 1; i.e., a value of 1 indicates that cell faces are flat whereas lower values indicate that the solid phase presents some degree of corrugation.

$$\frac{\sigma_c}{E_s} = \frac{1}{12}\left[\frac{2\pi(1-f_s)B}{C}\right]^2\left(\frac{\rho_f}{\rho_s}\right)^2\xi \tag{7}$$

Then, a simple way to estimate this corrugation ratio is to compare the experimental values of the collapse stress (σ_c^{exp}) with the theoretical values given by Eq. (4) (σ_c^{theo}), as indicated in Eq. (8).

$$\xi = \frac{\sigma_c{}^{exp}}{\sigma_c{}^{theo}} \tag{8}$$

2.4.2. Experimental measurement of the collapse stress

In order to measure experimentally the collapse stress of the materials under study a collection of compressive mechanical tests have been carried out by using a universal testing machine (Mod. 5.500R6025, INSTRON) at room temperature (25 °C) and low deformation rate. At these experimental conditions, the required stress (σ) in order to achieve a determined strain (ε) is calculated by the following expression [34]:

$$\sigma = \sigma_c + \frac{p_{atm}\varepsilon(1-2\nu)}{1-\varepsilon-{}^{\rho_f}/_{\rho_s}} \tag{9}$$

where p_{atm} is the atmospheric pressure during the experiment and ν is the material Poisson' ratio. A typical stress-strain curve of this type of materials (sample LDPE-3) is shown in Fig. 4(a). The collapse stress can be measured as the intercept of the straight line with the y axis when plotting the stress in the post collapse zone (strain from 0.2 to 0.5) versus $\varepsilon/(1-\varepsilon-\rho_f/\rho_s)$ (so-called volumetric strain) as it is shown in Fig. 4(b).

2.5. Thermal expansion coefficient

On the other hand, linear thermal expansion coefficient has been determined by Eq. (10):

$$\alpha = \frac{1}{l_0}\frac{dl}{dT} \tag{10}$$

where l_0 is the original length (or height) at a reference temperature (25 °C in this work) and l is the length (or height) of the sample at temperature T. It is known that this parameter is very sensitive to the

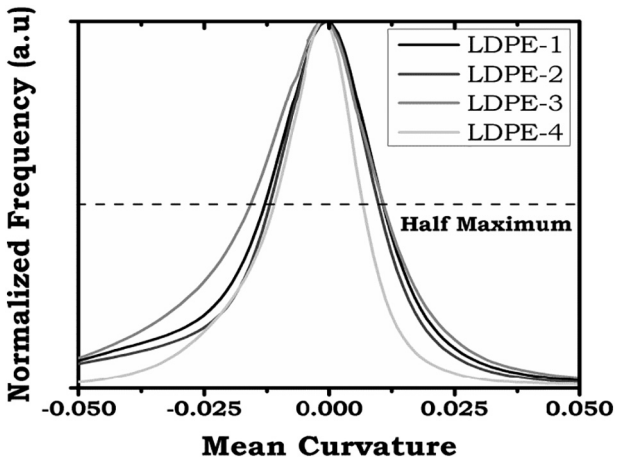

Fig. 6. Mean curvature distributions for the four analysed cellular materials.

Table 2
Summary of results onsolid phase corrugation for the materials under study.

Sample	Additional surface (*AS*) (%)	Curvature variation (*CV*)
LDPE-1	4.74 ± 0.38	0.02377
LDPE-2	4.30 ± 0.3	0.02180
LDPE-3	4.84 ± 0.5	0.02666
LDPE-4	3.87 ± 0.26	0.01783

presence of wrinkles in the structure of elastic cellular polymers [3]. As it will be shown in the results section, by analysing the variation of this parameter at 25 °C it is possible to elucidate the presence of cell-wall wrinkles and determine an approximate magnitude of corrugation in the solid phase of these materials. The enclosed-gas suffers a pressure increase due to the temperature rise which promotes that the wrinkles of the structure disappear at increasing temperature. This can be detected analysing the derivative value of the thermal expansion coefficient at temperature near 25 °C, i.e. the punctual slope of the thermal expansion coefficient at 25 °C. This temperature is selected since it corresponds to the temperature at which synchrotron μ-CT and mechanical tests were performed.

In our case, the thermal expansion coefficient has been experimentally determined by using a thermo-mechanical analyser (TMA, Perkin-Elmer TMA7) equipped with quartz parallel plate probe in order to measure the material changes in height over a temperature range from −20 °C to 100 °C with a heating rate of 3 °C/min. The analysed samples in this case where cylinders of 10 mm in diameter and 10 mm in height. In addition, at least three different experiments for each foam sample were carried out. Fig. 5 shows a typical thermal expansion curve (sample LDPE-1) of normalized sample length (l/l_0) and the linear thermal expansion coefficient (calculated using Eq. (10)) as a function of temperature.

3. Results and discussion

3.1. Solid phase corrugation

As mentioned above in the manuscript, two different methods of analysis for the solid phase corrugation have been employed. On one hand, mean curvature distributions of three different volumes of interest for each material have been suitably averaged. These histograms are shown in Fig. 6. All the curves presented a slight asymmetry to negative values due to the concavities of the cells in the material. In this case, we have defined the Curvature Variation (*CV*) as the parameter characterizing the solid phase corrugation. This parameter corresponds to the full-with at half-maximum (*FWHM*) of the mean curvature

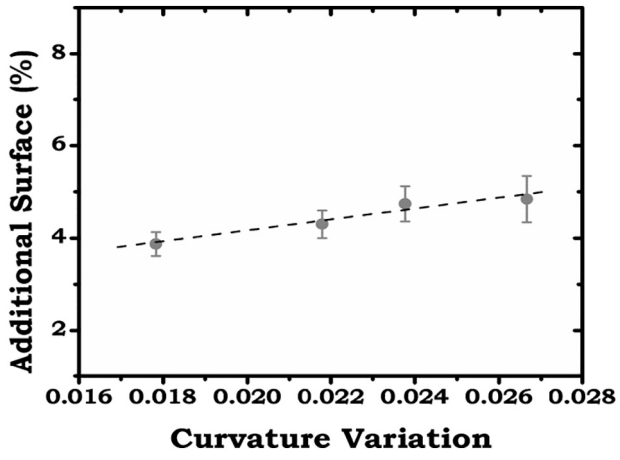

Fig. 7. Relationship between the *AS* and *CV*, the two parameters extracted from the tomographic data and used to quantify the solid phase corrugation.

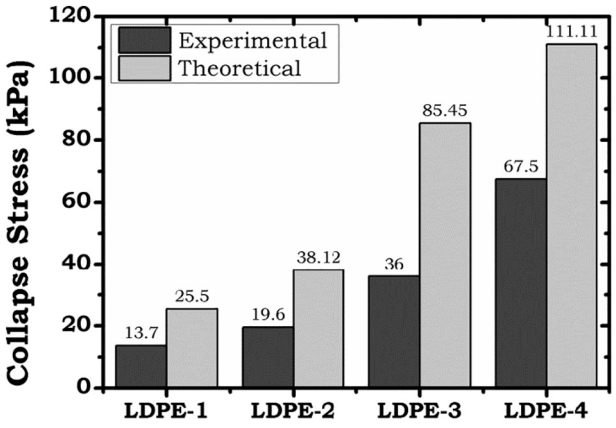

Fig. 8. Experimental and theoretical values of collapse stress.

histograms. A higher degree of corrugation in the solid structure promotes a wider curvature distributions and vice versa. Table 2 shows the results for this selected corrugation indicator. There is a clear difference between materials (up to 34% between LDPE-3 and LDPE-4).

In addition, Table 2 shows the obtained values for the Additional Surface (*AS*). Once again, differences between materials can be appreciated, although the maximum differences are smaller (23% between LDPE-3 and LDPE- 4).

It is important to mention that both parameters are directly correlated, as demonstrated in Fig. 7. According to the results, *AS* parameter is less sensitive to changes than *CV*, with nearly 30% higher maximum variation.

3.2. Collapse stress

The relation between the experimental and theoretical values of collapse stress (corrugation ratio) is determined in this section and compared with the geometrically-extracted parameters. To this end, experimental values are determined as explained in Section 2.4.2. Moreover, the theoretical values of collapse stress are calculated using Eq. (6) and considering the Young modulus of the solid LDPE, E_s, of 200 MPa. Both theoretical and experimental values of collapse stress are presented in Fig. 8.

As a consequence, the defined corrugation ratio (Eq. (8)) for the analysed samples takes values between 0.4 (LDPE-3) to 0.6 (LDPE-4). Fig. 9 shows that there is clear relation between the corrugation ratio and both Additional Surface and Curvature Variation. In the proposed trend (dashed line) the corrugation ratio tends to one when the *CV* tends to zero. A very similar trend is also observed for *AS* parameter including the validation that corrugation ratio tends to one when *AS* tends

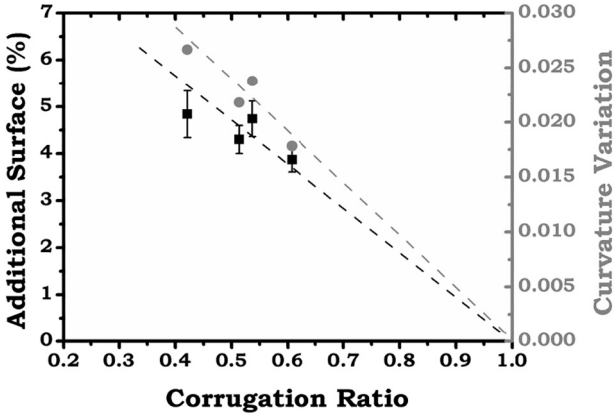

Fig. 9. Experimental relationship of corrugation ratio with *AS* and *CV*.

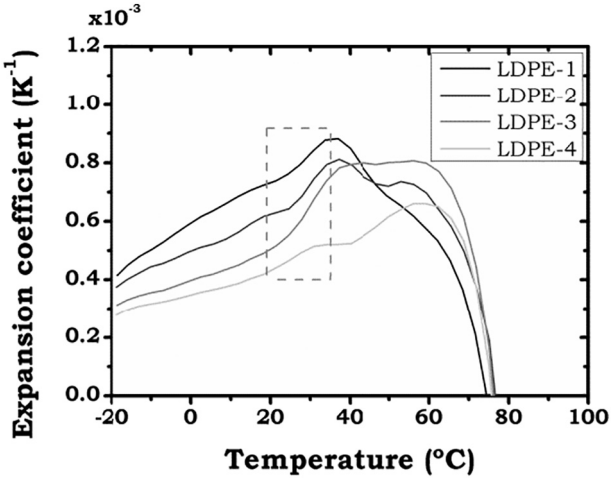

Fig. 10. Thermal expansion coefficient values of the analysed samples. The dashed square marks the temperature region in which the cell-wall flattening is taking place.

to 0. Both parameters are equally correlated with corrugation ratio. These results confirm our hypothesis; the solid phase corrugation is playing a clear role on the collapse stress of the foams.

3.3. Thermal expansion coefficient

Fig. 10 shows the results thermal expansion coefficient for all the materials under study. In all cases, the absolute value of thermal expansion coefficient for each temperature value is inversely related with the density of the foamed materials due to the higher gas volume percentage and the higher capacity of expansion of this gaseous phase in comparison with the solid phase [3,35]. For this reason, the higher thermal expansion coefficients are observed for LDPE-1 (density 16.4 kg/m^3) whereas the lower values are for LDPE-4 (density 41.3 kg/m^3). This tendency is maintained almost up to 40 °C. At temperatures above that values do no follow a clear trend since the polymeric matrix softens and other effects take place.

The slope of the thermal expansion coefficient curve at 25 °C is determined to evaluate the influence of solid phase corrugation on thermal expansion coefficient. The results of this analysis can be observed in Fig. 11. The material showing the greatest slope of the thermal expansion coefficient corresponds with the material with the highest solid phase corrugation, being therefore sample LDPE-3, whereas sample LDPE-4, which is the sample with the less corrugated structure, is the sample with a lower variation of thermal expansion coefficient at the mentioned temperature.

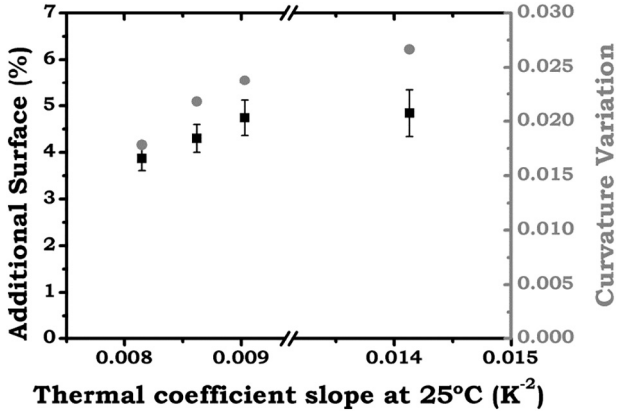

Fig. 11. Dependence of thermal expansion coefficient slope at 25 °C with *AS* and *CV*.

As it has been previously discussed the parameter *CV* allows obtaining higher differences between materials than the *AS* (34% of variation vs 23%) and seems to be slightly better correlated. As a consequence, this parameter is a more sensitive indicator of corrugations than the Additional Surface. For this reason, we consider that Curvature Variation is the most recommended microstructural indicator of solid phase corrugation. It has also to be taken into account inherent technical (synchrotron μ-CT at 0.438 μm resolution) and computational (complex computation method, long computing times) difficulties to determine it.

4. Conclusions

We have determined the effect of solid phase corrugation in low density flexible foams on two representative physical properties, the collapse stress and the thermal expansion coefficient. To this end, two different image analysis protocols applied to synchrotron μ-CT data sets with enough spatial resolution were developed. The two parameters defined to evaluate the solid phase corrugation are the Additional Surface, linked to the surface of the real cell in comparison to a model cell with the same volume but with flat cell walls and the Curvature Variation which corresponds to the FWHM of mean curvature distributions. It has been proved that these two parameters are mutually correlated and that Curvature Variation is slightly more sensitive to the presence of wrinkled cell walls in these foam specimens.

The results obtained for these two parameters can be well correlated with the two physical properties selected. An increase of the solid phase corrugation reduces the collapse stress of the foams and increases the slope of the thermal expansion curve at a temperature of 25 °C.

CRediT authorship contribution statement

S. Pérez-Tamarit: Conceptualization, Data curation, Formal analysis, Investigation, Methodology, Writing - original draft, Writing - review & editing. **E. Solórzano:** Conceptualization, Investigation, Supervision, Validation, Visualization, Writing - review & editing. **A. Hilger:** Data curation, Methodology, Software. **I. Manke:** Data curation, Methodology, Software. **M.A. Rodríguez-Pérez:** Conceptualization, Funding acquisition, Investigation, Methodology, Project administration, Resources, Supervision, Validation, Visualization, Writing - original draft, Writing - review & editing.

Acknowledgements

Financial assistance from MINECO, FEDER, UE (MAT2015-69234-R) and the Junta de Castile and Leon (VA011U16) are gratefully acknowledged. Predoctoral contract of S. Perez-Tamarit by University of Valladolid (E-47-2015-0094701) and co-financed by Banco Santander is also acknowledged. Finally, we acknowledge the support from Bessy II (HZB, Berlin, Germany) to complete this work (proposal 14100497-ST).

Data availability

The raw/processed data required to reproduce these findings cannot be shared at this time as the data also forms part of an ongoing study.

References

[1] L.J. Gibson, M.F. Ahsby, Cellular Solids: Structure and Properties. Pergamon Press, England, Oxford, 1988.
[2] M.A. Rodríguez-Pérez, Crosslinked polyolefin foams: production, structure, properties, and applications, Adv. Polym. Sci. 184 (2005) 97–126.
[3] O. Almanza, Y. Masso-Moreu, N.J. Mills, M.A. Rodríguez-Pérez, Thermal expansion coefficient and bulk modulus of polyethylene closed-cell foams, J. Polym. Sci. B Polym. Phys. 42 (2004) 3741–3749.
[4] D. Arencón, M. Antunes, V. Realinho, J.I. Velasco, Influence of chemical nature, expansion ratio and cellular morphology on the fracture behaviour of flexible polyolefin-based foams assessed by the essential work of fracture (EWF), Polym. Test. 43 (2015) 163–172.

[5] M.A. Spalding, A. Chatterjee, Handbook of Industrial Polyethylene and Technology: Definitive Guide to Manufacturing, Properties, Processing, Applications and Markets Set, Wiley, 2017.
[6] E.T. Bird, A.E. Bowden, M.K. Seeley, D.T. Fullwood, Materials selection of flexible open-cell foams in energy absorption applications, Mater. Des. 137 (2018) 414–421.
[7] N. Mills, Polymer foams for personal protection: cushions, shoes and helmets, Compos. Sci. Technol. 63 (2003) 2389–2400.
[8] V. Bernardo, E. Laguna-Gutierrez, A. Lopez-Gil, M.A. Rodriguez-Perez, Highly anisotropic crosslinked HDPE foams with a controlled anisotropy ratio: production and characterization of the cellular structure and mechanical properties, Mater. Des. 114 (2017) 83–91.
[9] A.N. Gent, A.G. Thomas, The deformation of foamed elastic materials, J. Appl. Polym. Sci. 1 (1959) 107–113.
[10] A.N. Gent, A.G. Thomas, Mechanics of foamed elastic materials, Rubber Chem. Technol. 36 (1963) 597–610.
[11] L.J. Gibson, Modelling the mechanical behavior of cellular materials, Mater. Sci. Eng. A 110 (1989) 1–36.
[12] S. Pardo-Alonso, E. Solorzano, J. Vicente, L. Brabant, M.L. Dierick, I. Manke, et al., muCT-based analysis of the solid phase in foams: cell wall corrugation and other microscopic features, Microsc. Microanal. 21 (2015) 1361–1371.
[13] A.E. Simone, L.J. Gibson, The effects of cell face curvature and corrugations on the stiffness and strength of metallic foams, Acta Mater. 46 (1998) 3929–3935.
[14] J.L. Grenestedt, Influence of wavy imperfections in cell walls on elastic stiffness of cellular solids, J. Mech. Phys. Solids 46 (1998) 29–50.
[15] D. Klempner, K.C. Frish, in: Hanser (Ed.), Handbook of Polymeric Foams and Foam Technology, 1991.
[16] E.M. Stokely, S.Y. Wu, Surface parametrization and curvature measurement of arbitrary 3-D objects: five practical methods, IEEE Trans. Pattern Anal. Mach. Intell. 14 (1992) 833–840.
[17] O. Almanza, M.A. Rodriguez- Perez, J.A. de Saja, The microestructure of polyethylene foams produced by a nitrogen solution process, Polymer 42 (2001) 7117–7126.
[18] S. Pérez-Tamarit, E. Solórzano, A. Hilger, I. Manke, M.A. Rodríguez-Pérez, Multi-scale tomographic analysis of polymeric foams: a detailed study of the cellular structure, Eur. Polym. J. 109 (2018) 169–178.
[19] A. Rack, S. Zabler, B.R. Müller, H. Riesemeier, G. Weidemann, A. Lange, et al., High resolution synchrotron-based radiography and tomography using hard X-rays at the BAMline (BESSY II), Nucl. Instrum. Methods Phys. Res., Sect. A 586 (2008) 327–344.
[20] https://www.fei.com/software/amira-avizo/.
[21] W.E. Warren, A.M. Kraynik, Linear elastic behavior of a low-density kelvin foam with open cells, J. Appl. Mech. 64 (1997) 787–794.
[22] H. Jinnai, T. Koga, Y. Nishikawa, T. Hashimoto, S.T. Hyde, Curvature determination of spinodal interface in a condensed matter system, Phys. Rev. Lett. 78 (1997) 2248–2251.
[23] D. Kammer, P. Voorhees, The morphological evolution of dendritic microstructures during coarsening, Acta Mater. 54 (2006) 1549–1558.
[24] O. Stein, E. Grinspun, K. Crane, Developability of triangle meshes, ACM Trans. Graph. 37 (2018) 1–14.
[25] E. Magid, O. Soldea, E. Rivlin, A comparison of Gaussian and mean curvature estimation methods on triangular meshes of range image data, Comput. Vis. Image Underst. 107 (2007) 139–159.
[26] J. Alkemper, P.W. Voorhees, Three-dimensional characterization of dendritic microstructures, Acta Mater. 49 (2001) 897–902.
[27] J. Lee, R.M. Nishikawa, I. Reiser, J.M. Boone, K.K. Lindfors, Local curvature analysis for classifying breast tumors: preliminary analysis in dedicated breast CT, Med. Phys. 42 (2015) 5479–5489.
[28] A. Lopez, K. Brodlie, Improving the robustness and accuracy of the marching cubes algorithm for isosurfacing, IEEE Trans. Vis. Comput. Graph. 9 (2003).
[29] W.E. Lorensen, H.E. Cline, Marching cubes: a high resolution 3D surface construction algorithm, Comput. Graph. 21 (1987).
[30] L. Zhao, X. Shi, H. Xia, The research of the digital core construction based on marching cubes, IOP Conference Series: Materials Science and Engineering, 394, 2018, p. 042065.
[31] L.J. Gibson, Biomechanics of cellular solids, J. Biomech. 38 (2005) 377–399.
[32] K.B. Bhagavathula, A. Azar, S. Ouellet, S. Satapathy, C.R. Dennison, J.D. Hogan, High rate compressive behaviour of a dilatant polymeric foam, J. Dyn. Behav. Mater. 4 (2018) 1–13.
[33] E. Laguna Gutiérrez, E. Solórzano, S. Pardo-Alonso, M.A. Rodriguez-Perez, Modelling the Compression Behaviour of Low-density Flexible Foams With a Partially Interconnected Cellular Structure, SPE FOAMS, 2012.
[34] Y. Masso Moreu, N.J. Mills, Rapid hydrostatic compression of low-density polymeric foams, Polym. Test. 23 (2004) 313–322.
[35] R. Lakes, Cellular solid structures with unbounded thermal expansion, J. Mater. Sci. Lett. 15 (1996) 475–477.